# Speed-Dependent Photofragment Orientation in the Photodissociation of OCS at 223 nm

**Zee Hwan Kim, Andrew J. Alexander, and Richard N. Zare***

*Department of Chemistry, Stanford University, Stanford, California 94305*

*Received: June 16, 1999; In Final Form: August 16, 1999*

Carbonyl sulfide (OCS) was photolyzed with linearly polarized 223 nm light and the sulfur-atom photofragment $S(^1D_2)$ was probed by (2 + 1) resonance enhanced multiphoton ionization (REMPI) using alternatively left and right circularly polarized light. The measured orientation of the angular momentum was found to depend strongly on the speed of the sulfur atom photofragment: fast S atoms show a large orientation, whereas slow S atoms show little or no orientation. Orientation results from quantum mechanical interference associated with mixed parallel $^1A'(^1\Delta)-^1A'(^1\Sigma^+)$ and perpendicular $^1A''(^1\Sigma)-^1A'(^1\Sigma^+)$ transitions that lead to the same photofragment state ($^1D_2$). Comparison of speed-dependent orientation with the expected envelope of the oscillation of the orientation suggests that the asymptotic phase differences of the two wave functions are nearly constant over different rotational states of the CO photofragment. This result can be explained by the similarity of the two potential energy surfaces involved.

## Introduction

The field of photodissociation dynamics, pioneered by Kent R. Wilson,[1] combines the power of molecular scattering experiment with the precision of laser spectroscopy. The photodissociation process can be viewed as a "half-collision" analogue of bimolecular reactive scattering. By using lasers with well-defined polarization and energy, the initial conditions of the half-collision can be extremely well-defined, giving much insight into the nature of excited-state dynamics. The measurement of angular momentum polarization, that is, the correlation of the angular momentum vector with the photofragment recoil velocity vector, has been proven to reveal additional information that is not available from other observables.[2] The angular momentum polarization is not lost by the formation of a long-lived excited-state complex and can provide information about the dynamics occurring beyond the Franck−Condon region. In 1968, Van Brunt and Zare[3] predicted that the photodissociation of a diatomic molecule may lead to polarized atomic photofragments. This prediction was based on the adiabatic correlation of the diatomic molecule to its separated atomic photofragments,[4] and on the axial recoil approximation.[5] The quantum mechanical nature of angular momentum polarization manifests itself in effects such as coherence and interference between the photofragment quantum states: these effects are more pronounced in the case of atomic photofragments partly owing to their low angular momentum quantum numbers. Full quantum mechanical treatments of photofragment polarization, allowing for mixed transitions and photofragment coherence, have been given by Vasyutinskii[6] and Siebbeles et al.[7] Several experiments have since demonstrated the polarization of atomic photofragments and quantum mechanical effects.[8−11]

Rakitzis and Zare[12] recently showed how to measure the complete photofragment angular momentum distribution using a specialized set of polarization parameters, $\boldsymbol{a}_q^{(k)}(\parallel)$, $\boldsymbol{a}_q^{(k)}(\perp)$, and $\boldsymbol{a}_q^{(k)}(\parallel,\perp)$. The $\boldsymbol{a}_q^{(k)}(\parallel)$ and $\boldsymbol{a}_q^{(k)}(\perp)$ parameters are associated only with the parallel and the perpendicular transitions, separately. The $\boldsymbol{a}_q^{(k)}(\parallel,\perp)$ parameters result from the coherence of the wave functions associated with dissociative states of differing symmetries. Experimentally, Rakitzis et al.[13,14] observed the orientation moment, $\mathrm{Im}[\boldsymbol{a}_1^{(1)}(\parallel,\perp)]$ of ground-state chlorine atoms in the photodissociation of ICl, which oscillates as a function of photolysis energy. These oscillations can be explained by quantum mechanical interference between the two repulsive-state wave functions associated with the mixed parallel and perpendicular transition. The orientation moment is proportional to sin $\Delta\phi$ where $\Delta\phi = \phi_\perp - \phi_\parallel$ is the asymptotic phase difference between the radial parts of the outgoing wave functions from the excited states associated with the parallel and perpendicular transitions, respectively. The orientation is also proportional to the product of transition dipole moments for these transitions:

$$\mathrm{Im}[\boldsymbol{a}_1^{(1)}(\parallel,\perp)] \propto |\mu_\parallel||\mu_\perp|\sin\Delta\phi \qquad (1)$$

where $|\mu_\parallel|$ and $|\mu_\perp|$ are the moduli of transition dipole moments for parallel and perpendicular transitions leading to the same product quantum states. For a pure (either parallel or perpendicular) transition, the product of the two amplitudes $|\mu_\parallel||\mu_\perp|$ is zero, and the value of $\mathrm{Im}[\boldsymbol{a}_1^{(1)}(\parallel,\perp)]$ vanishes. The asymptotic phase difference $\Delta\phi$ and hence the $\mathrm{Im}[\boldsymbol{a}_1^{(1)}(\parallel,\perp)]$ is sensitive to the detailed shapes of potential energy surfaces. Recently, we have shown that the measurement of the oscillating orientation moment of the atomic photofragment can probe nonadiabatic interactions in the photodissociation of $Cl_2$.[15]

The photodissociation dynamics of polyatomic molecules are much less understood than the photodissociation dynamics of diatomic molecules owing to the increased complexity associated with the additional degrees of freedom. Because of this increased dimensionality, it is not quite straightforward to interpret the result of conventional measurements (for example, the measurements of spatial anisotropies of the photofragments, product branching ratios and product state distributions). The measurement of the asymptotic phase relationship of the wave functions might open another dimension for the understanding of the complicated photodissociation dynamics. Only a few experi-

* To whom the correspondence should be addressed. E-mail: zare@stanford.edu. Fax: +1-650-725-0259.

10.1021/jp991988q CCC: $18.00 
Published on Web 10/14/1999

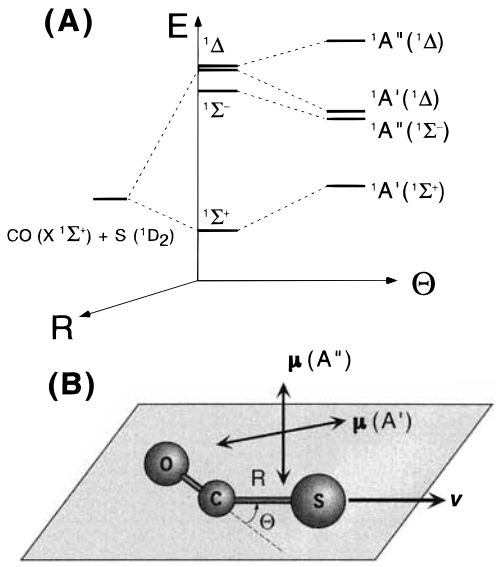


**Figure 1.** (A) Schematic diagram of the ground and excited states involved. (B) The transition dipole moments for parallel (in-plane) (A′−A′) and perpendicular (A″−A′) transitions. For perpendicular transition, the transition dipole is perpendicular to the molecular plane, for the parallel (in-plane) transition, the transition dipole is in the molecular plane, not necessarily being parallel to the direction of S−C bond.

mental observations of photofragment coherence in the photodissociation of triatomic molecules have been reported to date. Wittig and co-workers[16] as well as Zare and co-workers observed[17−19] the oscillation of the fine-structure branching ratio as a function of CN photofragment rotational quantum number[17] in the photodissociation of ICN. Zare and co-workers also observed the orientation[18,19] of the CN photofragment. It was suggested that these behaviors could be explained by quantum mechanical interference between two repulsive-state wave functions associated with the parallel and the perpendicular transitions.[17,20] More recently, Ahmed et al.[21] reported the observation of coherence in the alignment moment of O($^3$P) photofragments in the photodissociation of $NO_2$.

The photodissociation of carbonyl sulfide, OCS → CO(X $^1\Sigma^+$) + S ($^1D_2$,$^3P_{J=0,1,2}$) is an attractive candidate for studies of photofragment orientation and alignment. Sensitive detection schemes for both photofragments are available, and there is no nuclear spin angular momentum that might wash out[2] the initially prepared orientation and the alignment of photofragments. In addition, several intriguing observations have been made on this system in previous works. With a linear geometry, the ground state of OCS is characterized as $^1\Sigma^+$ and its low-lying excited states are $^1\Sigma^-$ and $^1\Delta$. The transitions to these two excited states are forbidden for the linear geometry, but weakly allowed for bent geometries. The $^1\Sigma^-$ excited state correlates to A″($^1\Sigma^-$), and the degenerate $^1\Delta$ excited state is split into a pair of A′($^1\Delta$) and A″($^1\Delta$) Renner−Teller states, whereas the ground state $^1\Sigma^+$ correlates to the A′($^1\Sigma^+$) state on bending (see Figure 1, A and B). Rabalais et al.,[22] using a Walsh diagram, showed that the A′($^1\Delta$) and A″($^1\Sigma^-$) states favor bent geometries whereas the A′($^1\Sigma^-$) and A″($^1\Delta$) states favor linear geometries. It is believed that the photodissociation near 223 nm is via dissociative A′($^1\Delta$) and A″($^1\Sigma^-$) states to give CO(X $^1\Sigma^+$) and S($^1D_2$; ∼95%) and S ($^3P_{J=0,1,2}$; ∼5%).[23−25] Sivakumar et al.[24] observed a bimodality in the CO product rotational state distribution with a major peak at $J = 57$ and a minor peak at $J = 70$ for photolysis of OCS at 222 nm. This high rotational excitation of the CO photofragment could not be understood by a simple impulsive model,[26] suggesting that the major contribution to the formation of rotationally hot CO photofragments arises from the bent excited states. The angular distribution of the CO photofragment gradually changes from almost isotropic ($\beta \sim 0$) to anisotropic ($\beta \sim 1.8$) in going from lower-$J$ to higher-$J$ CO photofragments. Sivakumar et al. attributed this gradual change of spatial anisotropy to mixed parallel A′($^1\Delta$) and perpendicular A″($^1\Delta$) transitions for the lower-$J$ CO distribution, and from a pure parallel transition for the higher-$J$ component of the CO distribution, possibly via the A′($^1\Delta$) state. Recently, Suzuki et al.[25] carried out a detailed study of OCS photodissociation dynamics at various wavelengths using the photofragment imaging technique. They reassigned the excited states involved as A′($^1\Delta$) and A″($^1\Sigma^-$) states based on the wavelength dependence of the spatial anisotropies of the fast component of S($^1D_2$) atom.

In this paper, we report the measurement of the speed-dependent orientation moment Im[$\boldsymbol{a}_1^{(1)}$(∥,⊥)] of the S($^1D_2$) atom photofragment in the photodissociation of OCS using linearly polarized 223 nm photolysis light and circularly polarized probe light. We show that the measured orientation moment of the fast component of S($^1D_2$) atom is caused by quantum mechanical interference between the parallel and the perpendicular transitions whose excited states correlate to the same separated photofragment states.

## Experimental Section

Detailed descriptions of the experimental apparatus and techniques have been given elsewhere,[13,27] and only a brief overview is given here. Carbonyl sulfide (Matheson, 99.8%) was premixed with high-purity helium (Liquid Carbonic, 99.995%) to make a dilute mixture (ca. 5 vol %) before supersonic expansion through a pulsed nozzle (General Valve 9-Series, 0.6 mm orifice) into high vacuum. The stagnation pressure of the sample was kept below 100 Torr to prevent the formation of clusters. The 223 nm photolysis light was generated by mixing the frequency-doubled output of a dye laser pumped by a $Nd^{3+}$:YAG laser (Continuum, ND6000 and PL9020) with the residual fundamental (1064 nm) output of the $Nd^{3+}$:YAG laser. The probe light (291.48 nm) for 2 + 1 REMPI detection of S($^1D_2$) via the $3s^23p^3(^2D°)4p\ ^1P_1-3s^23p^4\ ^1D_2$ transition was generated by frequency doubling the output of a dye laser pumped by a second $Nd^{3+}$:YAG laser (Spectra-Physics, PDL-3 and DCR-2A). The spatial anisotropy of CO($X^1\Sigma^+$) was obtained by 2 + 1 REMPI via the Q-branch members of the B $^1\Sigma^+-X\ ^1\Sigma^+$ transition. Photolysis and probe beams were loosely focused onto the unskimmed expansion within the extraction region of a Wiley-McLaren time-of-flight (TOF) mass spectrometer operated under velocity-sensitive conditions. A core extractor was placed in front of the microchannel plates (MCP) preferentially to collect ions flying along the time-of-flight axis. Unlike photodissociation of diatomic molecules in which the atomic photofragment has a single speed, the S-atom photofragment assumes a distribution of speeds. Core extraction enhances sensitivity to the velocity-resolved polarization moment. The intensities of the photolysis and probe beams were attenuated to avoid unwanted distortion of TOF profiles caused by space charge effects.

Circular polarization of the probe radiation was achieved by placing a Soleil−Babinet compensator (Special Optics) with its optical axis at 45° with respect to the linear polarization vector of the probe UV light. A photoelastic modulator (PEM, Hinds International, PEM-80) was placed in front of the Soleil−Babinet compensator to flip the polarization to be either left-circularly polarized (LCP) or right-circularly polarized (RCP)

with respect to the propagation axis of the beam on a every-other-shot basis. The absolute handedness of the circular polarization was determined by placing a single Fresnel rhomb after the Soleil−Babinet compensator and measuring the combined retardation. To achieve maximum sensitivity to the detection of the orientation moment, the polarization of the pump laser was tilted by 45° with respect to the TOF detection axis using a double Fresnel rhomb (Optics for Research, RFU-1/2-U). The time delay between photolysis and probe pulses was kept within 20 ns to avoid unwanted fly-out of photofragments from the detection region. Purity of polarization was found to be critical for these experiments, and therefore care was taken to avoid distortions of the polarization of both photolysis and probe beams. TOF profiles taken using left-circularly polarized probe light $\mathbf{I}_{LCP}$ and right-circularly polarized probe light $\mathbf{I}_{RCP}$ were recorded separately on a shot-to-shot basis. Isotropic ($\mathbf{I}_{ISO} = \mathbf{I}_{LCP} + \mathbf{I}_{RCP}$), and anisotropic ($\mathbf{I}_{ANISO} = \mathbf{I}_{LCP} - \mathbf{I}_{RCP}$) composite TOF profiles were calculated and the orientation moments were extracted by fitting of these profiles.

Isotropic and anisotropic basis functions, $\mathbf{B}_{ISO}(v_i)$ and $\mathbf{B}_{ANISO}(v_i)$, were generated by a Monte-Carlo simulation described in Rakitzis and Zare,[12] where $v_i$ is *i*th component in the velocity distribution. Experimental composite TOF profiles $\mathbf{I}_{ANISO}$ and $\mathbf{I}_{ISO}$ are least-squares fitted using the following equations:

$$\mathbf{I}_{ISO} = \sum_i c_i \mathbf{B}_{ISO}(v_i) \tag{2}$$

$$\mathbf{I}_{ANISO} = \sum_i c_i \, \mathrm{Im}[\boldsymbol{a}_1^{(1)}(v_i)] \mathbf{B}_{ANISO}(v_i) \tag{3}$$

The $c_i$ are determined by fitting eq 2 first, and represent the velocity distribution of the S-atom photofragment in the absence of any orientation moment. To avoid spurious oscillations in the fitting parameters caused by the covariance between speed components of the basis set, the number of speed components chosen for the fitting was minimized. The S-atom speed-dependent spatial anisotropy $\beta(v)$ needed for generating the basis functions was obtained by interpolating the spatial anisotropy measured for the CO photofragments, $\beta(J)$. The fitting procedures were found to be insensitive to small variations (ca. 5%) in the $\beta$ parameter. The sensitivity of the atomic REMPI transition to orientation was calculated using the method of Mo et al.[11] ($s_1 = -5/\sqrt{6}$, following the notation of Rakitzis et al.[28]).

## Results

**Spatial Anisotropy.** Instead of directly measuring the speed-dependent spatial anisotropy of S($^1D_2$) atomic photofragments, the spatial anisotropies of CO photofragments in various rotational states were measured by 2 + 1 REMPI of the Q-branch members of the B $^1\Sigma^+$−X $^1\Sigma^+$ transition. This transition is of Σ−Σ type and it is known to have very low sensitivity to the orientation and alignment in the two-photon absorption,[29] so that it provides an alignment-free measurement of the spatial anisotropy. Figure 2 shows the measured spatial anisotropy as a function of rotational state of CO photofragments. Our measurements of the CO rotational state dependent spatial anisotropy are in reasonable accord with those previously published.[11,24,25] At higher rotational state, $J \sim 65$, angular distribution shows almost parallel ($\beta \sim 1.8$) character, and at lower rotational state, $J \sim 54$, the distribution shows an almost isotropic ($\beta \sim 0.35$) distribution. In the intermediate region ($J = 63-57$), the $\beta$ parameter changes rapidly from an anisotropic to an isotropic distribution. At lower rotational state, $J \sim 54$, corresponding to the S($^1D_2$) atom speed of 1.2 km/s, our measurement ($\beta \sim 0.35$) shows appreciable difference from those measured by Suzuki et al. ($\beta = 0.7$), and by Sivakumar et al. ($\beta \sim 0.1$). This discrepancy may be caused by the signal from the probe light (~229.9 nm) background in our measurement.[30]

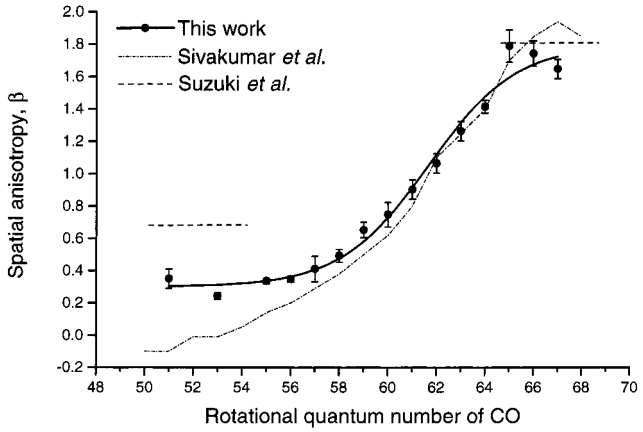


**Figure 2.** Spatial anisotropy of CO(X $^1\Sigma^+$) photofragment (filled circles) as a function of rotational quantum state obtained by 2 + 1 REMPI of the Q-branch members of the B $^1\Sigma^+$−X $^1\Sigma^+$ transition. Solid line is a fit of the $\beta$ parameters with sigmoidal function. The interpolated curve was constrained to have a limiting value of 1.8 and 0.3 at high and low limiting rotational quantum numbers, respectively. Also shown are the $\beta$ parameters for the fast and slow components of S($^1D_2$) atom by Suzuki et al.[25] (dashed lines), and the $\beta$ parameters of CO photofragments measured by Sivakumar et al. [24] at 222 nm (dash−dot line). See text for details.

**Speed-Dependent Orientation Moment.** In Figure 3A, we show core-extracted time-of-flight profiles of the S($^1D_2$) atom taken with left-circularly polarized (LCP) probe light and right-circularly polarized (RCP) probe light. We can easily identify the bimodality of the speed distribution from the TOF profiles: the fast and slow components have speeds of 1.2 and 0.8 km/s, respectively. Without any quantitative analysis, it is very clear that the TOF profile taken with RCP probe light has a significantly larger fast component than the one taken with LCP probe light. This observation suggests that only the fast components of the S-atom speed distribution are significantly oriented. For a quantitative analysis of the speed-dependent orientation moment, both the isotropic and the anisotropic components of the TOF profiles were fitted simultaneously, as described in the Experimental Section. Figure 3B shows the fit of the isotropic and anisotropic components of the TOF profiles. The speed distribution and the speed-dependent orientation moment of the S($^1D_2$) atom obtained by the fitting are shown in Figure 4A. The speed distribution possesses a major peak at 1.2 km/s and a minor peak at 0.8 km/s, in good agreement with previous studies.[11,24,25] The orientation moment, $\mathrm{Im}[\boldsymbol{a}_1^{(1)}(\|,\perp)]$ of the S($^1D_2$) atom shows an interesting speed dependence (see Figure 4B): the orientation moment in the speed range of 400−1000 m/s is relatively small. The orientation moment begins to grow at 1000 m/s until it finally reaches a somewhat constant positive value at around 1300 m/s. The orientation moment does not show any oscillation as a function of S-atom speed, in constrast to the case of CN photofragments measured in the photodissociation of ICN.[17] If we assume that the orientation moment of the S($^1D_2$) atom originates from a mixed parallel and perpendicular transiton and also assume that measured spatial anisotropy is the weighted (incoherent) average of

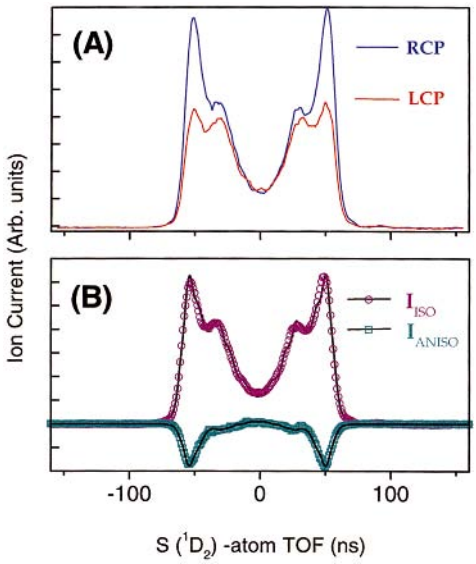


**Figure 3.** (A) Time-of-flight (TOF) profiles of S($^1D_2$) taken with left-circularly polarized (LCP, red) and right-circularly polarized (RCP, blue) light. Bimodal speed distribution centered at 1.2 and 0.8 km/s can be clearly identified. Note the large (~50%) enhancement of the fast component of TOF profiles taken with RCP probe light, showing that the fast component of the speed distribution is oriented with respect to the recoil velocity vector. (B) Isotropic and anisotropic TOF profiles. Open circles represent isotropic ($\mathbf{I}_{ISO} = \mathbf{I}_{LCP} + \mathbf{I}_{RCP}$) component of TOF profile; open squares correspond to the anisotropic ($\mathbf{I}_{ANISO} = \mathbf{I}_{LCP} - \mathbf{I}_{RCP}$) component of TOF profile. Also shown are the results of fitting with multiple-speed basis set generated by Monte-Carlo simulation (solid lines).

limiting $\beta$ parameters for the parallel and the perpendicular transition, we can model the factor, $|\mu_\parallel||\mu_\perp|$ (see eq 1) of the Im[$\boldsymbol{a}_1^{(1)}$(∥,⊥)] in terms of speed-dependent spatial anisotropy, $\beta(v)$:

$$A_\beta(v) = [(1.8 - \beta(v))(1 + \beta(v))]^{1/2} \propto |\mu_\parallel||\mu_\perp| \qquad (4)$$

where $A_\beta(v)$ is the envelope of photofragment orientation with speed $v$. In this expression, we assume that the "in-plane" transition dipole moment [A′($^1\Delta$)−A′($^1\Sigma^+$)] is associated with an anisotropy parameter of $\beta = 1.8$. The envelope $A_\beta(v)$ shown in Figure 4C has a speed dependence qualitatively similar to the measured orientation moment. The similarity between the measured orientation moment and the modeled envelope based on the assumption of a mixed parallel and perpendicular transition reveals two important points. First, this behavior affirms our assumption of a mixed transition for the fast component of the S-atom speed distribution, which shows that the orientation of the S atom is caused by the interference between the parallel and the perpendicular transitions. Second, the observation that the orientation moment does not show any oscillatory structure implies that the asymptotic phase difference between the two repulsive-state wave functions is nearly constant at this photolysis wavelength.

## Discussion

The speed-dependent spatial anisotropy of the S($^1D_2$) atom, $\beta(v)$, has been explained[24] by a mixed parallel [A′($^1\Delta$)−A′($^1\Sigma^+$)] and perpendicular [A″($^1\Sigma^-$)−A′($^1\Sigma^+$)] transition for the fast component of the bimodal distribution, the slow component originating from a transition with a parallel character, possibly via the A′($^1\Delta$) state. This postulate is based on the reasonable assumption that the dissociation process is instantaneous and the direction of the transition dipole moment for

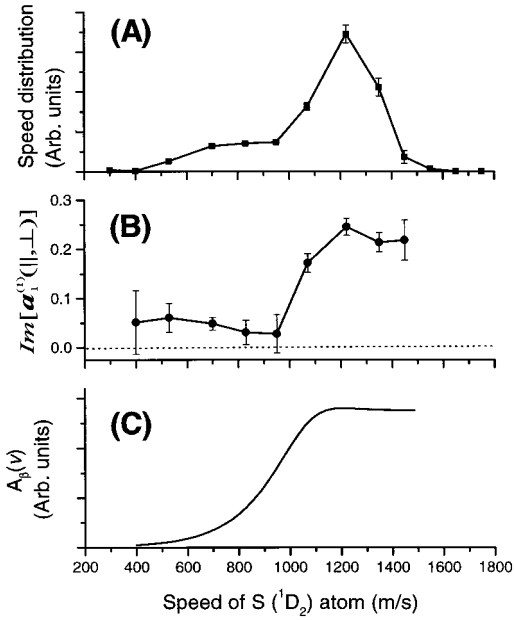


**Figure 4.** (A) Speed distribution (filled squares) of S($^1D_2$) photofragment. (B) The speed-dependent orientation (filled circles) Im[$\boldsymbol{a}_1^{(1)}$(∥,⊥)]. There is no or little orientation for the slow (~0.8 km/s) component whereas the fast (1.2 km/s) component shows large orientation. The error bars represent the 1 standard deviation of the result of the multiple measurements. (C) The modulation amplitude modeled by $A_\beta(v) = [(1.8 - \beta(v))(1 + \beta(v))]^{1/2}$. This modeled amplitude has a shape similar to the measured speed-dependent orientation moment of the S atom.

the in-plane transition (A′−A′) is approximately parallel to the recoil direction of the S($^1D_2$) atom (i.e., $\beta \sim 2$). Recent work by Suzuki et al.[25] shows a gradual change of the $\beta$ parameter for the fast component of the S-atom velocity distribution from $\beta \sim 0$ to $\beta < 0$ as the excitation wavelength is tuned from 223 to 248 nm. Again, this finding supports the suggested mechanism of a mixed transition. If we accept the postulated mechanism of the speed-dependent $\beta$ parameter, our observation is completely consistent with our picture of the physical origin of the orientation moment, $\beta$ parameter trends, and the proposed mixed transition mechanism. It would be expected that the fast component, which originates from a mixed transition, would show a significant orientation moment. In contrast, the slow component, which has a nearly pure parallel character, should show little or no orientation, in good agreement with our observations.

An alternative mechanism for the observation of orientation in the photodissociation of a bent triatomic molecule might originate from coherence between the (parallel and perpendicular) projections of the in-plane transition [A′($^1\Delta$)−A′($^1\Sigma^+$)] dipole moment onto the recoil velocity vector of the photofragment, as was recently suggested by Ahmed et al.[21] in the case of photodissociation of $NO_2$. For this mechanism, the coherence, and hence the orientation moment, is completely determined by the geometry of the nuclei and the relative orientation of the transition dipole moment with respect to the recoil velocity vector of the photofragment. Therefore, the orientation moment arising from this mechanism does not carry information on the interference of the wave functions on different repulsive potential energy surfaces. In the OCS photodissociation, the Franck−Condon region of the transition is located slightly away from the linear configuration, and the orientation of the in-plane transition dipole moment may not be perfectly parallel with the recoil velocity vector of the S-atom photofragment. Therefore, it is probable that coherence origi-

nating purely from the in-plane $A'(^1\Delta)-A'(^1\Sigma^+)$ transition contributes to the orientation moment. The contribution from this mechanism will be proportional to $|\mu_x(A')||\mu_z(A')|$, where $\mu_x(A')$ and $\mu_z(A')$ are the projections of in-plane transition dipole moment $\mu(A')$ onto the *x*-axis (perpendicular to recoil direction) and the *z*-axis (parallel to the recoil direction), respectively. This contribution will not necessarily follow the change of spatial anisotropy of the photofragment. However, the measured orientation moment closely follows the envelope expected from the mixed transition. Therefore, we believe that the orientation moment originates mostly from the mixed transition, and hence, contains information on the asymptotic phase relationship of the two repulsive-state wave functions. The fact that the orientation moment closely follows the expected envelope implies that the phase difference $\Delta\phi$ is more or less constant over the fast component of the S-atom speed distribution that is associated with at least 10 different rotational states of CO photofragments. The constant or slow variation of phase difference $\Delta\phi$ across a range of rotational quantum states is a somewhat unexpected observation, considering the multidimensional character of the potential energy surface.

One explanation can be given in terms of the similarity of potential energy surfaces of $^1A''(^1\Sigma^-)$ and $^1A'(^1\Delta)$:[25] the $^1A''(^1\Sigma^-)$ state arises from the $(3a'')^1(13a')^1$ electronic configuration and the $^1A'(^1\Delta)$ state from the $(12a')^1(13a')^1$ electronic configuration. The 3a″ orbital correlates with the $3\pi_y^*$(S−C) antibonding orbital and 12a′ correlates with $3\pi_x^*$(S−C) antibonding orbital, where the *y*-axis is perpendicular to the molecular plane and the *x*-axis is in the molecular plane and perpendicular to the S−C bond. These orbitals are degenerate in a linear geometry and are known to have localized electron density on the S atom. Therefore, these orbitals remain close in energy on bending and on stretching of the S−C bond. The localized character of the 3a″ and 12a′ orbitals causes the similarity of the potential energy surfaces of the $^1A''(^1\Sigma^-)$ and $^1A'(^1\Delta)$ states. The resemblance between the two potential energy surfaces causes the pathways taken by the two wave functions leading to the same rotational state to be similar. Also, the similarity of the potential energy surfaces causes the average potential energy difference, $\Delta V$, to be small compared with the translational energy available to the photofragment. These two factors lead to the fairly constant asymptotic phase difference across the rotational distribution of the photofragments.

## Summary and Conclusions

We have observed the speed-dependent orientation moment of $S(^1D_2)$ photofragment in the photodissociation of OCS at 223 nm. The coherence of $S(^1D_2)$ atom photofragments originates from the interference between the parallel and the perpendicular transitions. The speed dependence of the orientation moment suggests that the asymptotic phase differences of the wave functions are fairly constant over the fast component of the S atom photofragments, which can be explained by the similarity of the two potential energy surfaces involved in the excitation. Given the complexity of the multiple state polyatomic photodissociation processes, the ability to measure the asymptotic phase relationship of repulsive-state wave functions promises special insight into the photodissociation dynamics of this polyatomic molecule not readily discernible from the measurement of other parameters.

**Acknowledgment.** The funding for this work by the U.S. National Science Foundation under grant No. CHE-99-00305 is gratefully acknowledged.

## References and Notes

(1) See, for example: Busch, G. E.; Mahoney, R. T.; Morse, R. I.; Wilson, K. R. *J. Chem. Phys.* **1969**, *51*, 837. Busch, G. E.; Wilson, K. R. *J. Chem. Phys.* **1972**, *56*, 3626. Busch, G. E.; Wilson, K. R. *J. Chem. Phys.* **1972**, *56*, 3638. Busch, G. E.; Wilson, K. R. *J. Chem. Phys.* **1972**, *56*, 3655.

(2) Orr-Ewing, A. J.; Zare, R. N. *Annu. Rev. Phys. Chem.* **1994**, *45*, 315.

(3) Brunt, R. J. V.; Zare, R. N. *J. Chem. Phys.* **1968**, *48*, 4304.

(4) Wigner, E.; Witmer, E. E. *Z. Phys.* **1928**, *51*, 859.

(5) Zare, R. N.; Herschbach, D. R. *Proc. I. E. E. E.* **1963**, *51*, 173−182.

(6) Vasyutinskii, O. S. *Opt. Spectrosk.* **1983**, *54*, 524.

(7) Siebbeles, L. D. A.; Glass-Maujean, M.; Vasyutinskii, O. S.; Beswick, J. A.; Roncero, O. *J. Chem. Phys.* **1994**, *100*, 3610.

(8) Rothe, E. W.; Krause, U.; Duren, R. *Chem. Phys. Lett.* **1980**, *72*, 100.

(9) Vigué, J.; Gangier, P.; Roger, G.; Aspect, A. *J. Phys. Lett. (Fr.)* **1981**, *42*, L531.

(10) Eppink, A. T. J. B.; Parker, D. H.; Janssen, M. H. M.; Buijsse, B.; van der Zande, W. J. *J. Chem. Phys.* **1998**, *108*, 1305.

(11) Mo, Y.; Katayanagi, H.; Heaven, M. C.; Suzuki, T. *Phys. Rev. Lett.* **1996**, *77*, 830.

(12) Rakitzis, T. P.; Zare, R. N. *J. Chem. Phys.* **1999**, *110*, 3341.

(13) Rakitzis, T. P.; Kandel, S. A.; Alexander, A. J.; Kim, Z. H.; Zare, R. N. *J. Chem. Phys.* **1999**, *110*, 3351.

(14) Rakitzis, T. P.; Kandel, S. A.; Alexander, A. J.; Kim, Z. H.; Zare, R. N. *Science* **1998**, *281*, 1346.

(15) Kim, Z. H.; Alexander, A. J.; Kandel, S. A.; Rakitzis, T. P.; Zare, R. N. *Faraday Discuss.* **1999**, *133*, in press.

(16) Shokoohi, F.; Hay, S.; Wittig, C. *Chem. Phys. Lett.* **1984**, *110*, 1.

(17) Joswig, H.; O'Halloran, M. A.; Zare, R. N.; Child, M. S. *Faraday Discuss.* **1986**, *82*, 79.

(18) Black, J. F.; Hasselbrink, E.; Waldeck, J. R.; Zare, R. N. *Mol. Phys.* **1990**, *71*, 1143.

(19) Hasselbrink, E.; Waldeck, J. R.; Zare, R. N. *Chem. Phys.* **1988**, *126*, 191.

(20) Vigué, J.; Girard, B.; Gouedard, G.; Billy, N. *Phys. Rev. Lett.* **1989**, *62*, 1358.

(21) Ahmed, M.; Peterka, D. S.; Bracker, A. S.; Vasyutinskii, O. S.; Suits, A. G. *J. Chem. Phys.* **1999**, *110*, 4115.

(22) Rabalais, J. W.; McModald, J. M.; Scherr, V.; McGlynn, S. P. *Chem. Rev.* **1971**, *71*, 73.

(23) Nan, G.; Burak, I.; Houston, P. L. *Chem. Phys. Lett.* **1993**, *209*, 383.

(24) Sivakumar, N.; Hall, G. E.; Houston, P. L.; Hepburn, J. W.; Burak, I. *J. Chem. Phys.* **1988**, *88*, 3692.

(25) Suzuki, T.; Katayanagi, H.; Nanbu, S.; Aoyagi, M. *J. Chem. Phys.* **1998**, *109*, 5778.

(26) Schinke, R. *Photodissociation Dynamics: Spectroscopy and Fragmentation of Small Polyatomic Molecules*; Wiley: New York, 1992.

(27) Simpson, W. R.; Orr-Ewing, A. J.; Kandel, S. A.; Rakitzis, T. P.; Zare, R. N. *J. Chem. Phys.* **1995**, *103*, 7299.

(28) Rakitzis, T. P.; Kandel, S. A.; Zare, R. N. *J. Chem. Phys.* **1997**, *107*, 9382.

(29) Bray, R. G.; Hochstrasser, R. M. *Mol. Phys.* **1976**, *31*, 1199.

(30) Photolysis at 229.9 nm produces the rotational distribution of CO with major peak at $J \sim 50$, whereas the major peak of the rotational distribution at 223 nm is located at $J \sim 55$. Therefore, the signal at $J \sim 50$ has a significant contribution from the probe background, which tends to reduce the value of measured $\beta$ parameter.